

New synthesis of hydroxyapatite from local phosphogypsum

H. Nasrellah¹, I. Yassine¹, B. Hatimi¹, M. Joudi¹, A. Chemaa¹, L. El Gaini²,
Z. Hatim¹, M.A. El Mhammedi³, M. Bakasse^{1*}

1. Laboratoire de Chimie Organique Bioorganique et Environnement, Faculté de Sciences,
Université Chouai Doukkali Morocco.

2. Laboratoire de Chimie Organique Appliquée, Faculté des Sciences Semlalia,
Université Cadi Ayyad, Marrakech, Morocco.

3. Univ Hassan1, Laboratoire de Chimie et Modélisation Mathématique,
Faculté Polydisciplinaire, 25000 Khouribga, Morocco.

Received 10 Jan 2017,
Revised 24 Apr 2017,
Accepted 28 Apr 2017

Keywords

- ✓ Moroccan phosphogypsum waste;
- ✓ New process;
- ✓ Hydroxyapatite;

M. Bakasse
minabakasse@yahoo.fr
+212662835969

Abstract

This present study relates a new process for direct synthesis of hydroxyapatite crystalline (HAP) from anhydrite extracted from Moroccan phosphogypsum (PG) waste. HAP was performed by reacting hydrated anhydrite with phosphoric acid in the presence of NaOH at low temperature in reactor elaborated in our laboratory. The proposed method leads to the obtaining of HAP with a Ca/P ratio equal to 1,667 which is close to 1,67 found in human bone and indicating stoichiometric HAP with a high degree of crystallinity, purity and a high yield. The advantage of this new process is to produce a crystalline HAP with particle size ranging from 0,1 to 0,4 μm and high free from Al, P, F, Si, Fe, Mg the most pollutant element that hinder the utilization of the PG waste. The provide HAP can be used for the treatment of liquid and gaseous effluents. The structural characteristics of HAP were determined by the X-ray diffraction (XRD), Fourier transform infrared spectroscopy (FT-IR) and Scanning Electron Microscopy-EDX.

1. Introduction

Phosphogypsum (PG) is a byproduct of wet-process phosphoric acid, a process in which phosphate rock is reacted with the sulfuric acid. Phosphogypsum is composed mainly of gypsum ($\text{CaSO}_4 \cdot 2\text{H}_2\text{O}$) which contains various harmful impurities of free phosphoric acid, phosphates, fluorides and organic matter that adhere to the surface of gypsum crystals and also substituted in the crystal lattice of gypsum [1,2]. For every ton of phosphoric acid produced, about three tons of phosphogypsum are generated. Morocco produces every year about 15 million tons of acid phosphogypsum residues which the vast majority is discharged into the sea [3]. The problems of pollution generated by this byproduct were discussed by many authors in the world [4,5]. The reuse solutions or recovery of such waste have also been proposed in other fields. Phosphogypsum was recycled as building materials, agricultural fertilizers or soil stabilization amendments and asset controller in the manufacture of Portland cement [6,7]. Treatment were also conducted to prepare hydroxyapatite nanoparticles from phosphogypsum [8,9]. Calcium hydroxyapatite $\text{Ca}_{10}(\text{PO}_4)_6(\text{OH})_2$ is one of the most important constituents of the biocompatible inorganic materials used in human hard tissues [10,11]. It has also been used in many industrial applications, such as catalysis, ion exchange, and metal removal [12-17]. Several techniques have been used to prepare calcium hydroxyapatite such as coprecipitation method [18,19], hydrothermal preparation [20]. These methods offer several advantages but consist of several steps, and remain time and energy consuming.

In the present work, we proposed a simple method to prepare stoichiometric calcium hydroxyapatite from Moroccan phosphogypsum waste with high yield, purity and nanoparticles for the treatment of the wastewater.

2. Experimental details

2.1. Raw materials

The PG waste derived from Moroccan phosphate rock was sampled from PG repository locations in the province of El Jadida, Morocco. The chemical composition of the PG was evaluated using the ICP spectroscopy and the results are presented in Table1.

Table 1: Chemical composition of phosphogypsum derived from Moroccan phosphate (%)

Ca	S	P	C	Al	Fe	K	F	Mg	Na	Si	Color
23.05	18.04	0.40	0.14	0.07	0.58	0.14	0.12	0.10	0.10	0.25	Greenish yellow

2.2 Reactor homemade description

The reactor consists in a Teflon frame (Figure 1). It comprises a (1) motor which ensures vigorous agitation, (2) a ball bearing, (3) inlet and (5) outlet valves and (4) an axis of rotation made of steel covered with polyethylene material which has a resistance to acid and alkaline media. The effective volume of the reactor is 2L. The present reactor assumes perfect mixing.

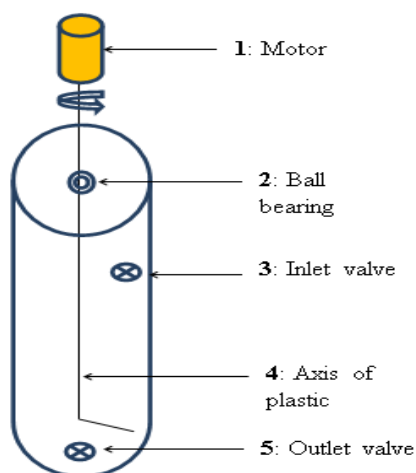


Figure 1: Schema of reactor used for synthesis of HAP from PG.

2.3 Preparation of the stoichiometric HAP powder

Method of preparation of HAP powder is shown in figure 2. In our previous work [21], the anhydrite crystal is first obtained through dehydration of phosphogypsum in strong sulfuric acid 67%. The cake is washed by water, washed by acetone, dried at 65°C and the final anhydrite product is obtained after a wet sieving using a 40 µm sieve.

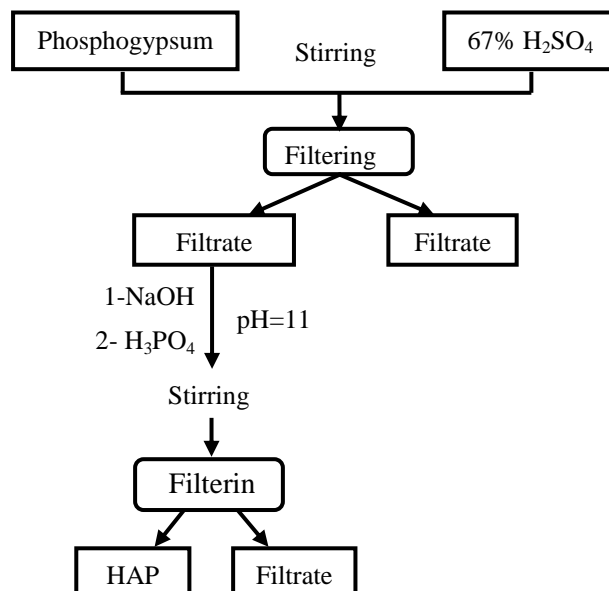


Figure 2: Diagram of preparing HAP particles from Moroccan PG.

Chemical analysis of the obtained anhydrite is shown in table 2. We can see that the percentage of all elements compared with those obtained in phosphogypsum decrease significantly except for sulfate and lime where we saw a slight increase because of probably dehydration of phosphogypsum to anhydrite.

Table 2: Chemical compositions of the obtained anhydrite

Ca	S	P	C	Al	Fe	Mg	Si	Color
40.28	57.50	0.20	0.0096	0.01	0.04	0.09	0.72	White

Then 10 g of anhydrite was added to a solution of sodium hydroxide in 100 ml of distilled water to adjust pH to 11. To this mixture 3ml of phosphoric acid 85% was slowly added under vigorous stirring. The product was maintained under a mechanical shaking during 48 hours. Crystals of stoichiometric HAP $\text{Ca}_{10}(\text{PO}_4)_6(\text{OH})_2$ immediately began to form. The precipitation continued until the supply in H_3PO_4 was exhausted. After 48 hours of mechanical agitation, the white suspension formed was separated from the solution and washed by distilled water up to the neutralization of the pH. The resulting stoichiometric HAP was dried at 105°C and calcined at 600°C and 900°C for 3h. Reaction of HAP formation can be expressed as follows:



2.4. Materials characterizations

The structure was examined with a PANalytical X-Pert Pro Multi-Purpose Diffractometer (MPD) using $\text{Cu K}\alpha$ radiation ($\lambda=1.54 \text{ \AA}$) at a scanning rate of $0.02^\circ/\text{s}$ for a range of $5\text{--}80$. The morphological surface characterization was performed by Field Emission Scanning Electron Microscopy (SEM) and Energy Dispersive X-ray Spectroscopy (EDS) conducted in a FEI (model Quanta FEG 450) microscopy operated at 20 kV. Transmittance IR spectra were recorded by Fourier Transform Infrared radiation using Shimadzu make FTIR-8400S series spectrophotometer at a resolution of 4 cm^{-1} and averaging over 25 scans in the range $400\text{--}4000 \text{ cm}^{-1}$. The inductively coupled plasma atomic emission spectroscopy (ICP–AES) measurements were performed with a Jobin Yvon ICP spectrometer (JY ULTIMA 2, plasma generator frequency 40.67 MHz), equipped with a cyclonic spray chamber and a concentric nebulizer. Quantification was done against standard calibration curve prepared with aqueous standards.

3. Results and Discussion

XRD patterns (Figure 3.a) of the obtained anhydrite show diffraction peaks characteristics anhydrite presents in standards and in literature [21]. The single phase, as expected, is anhydrite, which is confirmed by comparing data obtained with the standard JCPDS 00-037-1496 files.

The infrared spectroscopy analysis shows the presence of the characteristic bands of anhydrite (Figure 3.b) [21]. Bands at 601 and 667 cm^{-1} are attributed to the vibrations of symmetric and antisymmetric deformation of the ions (SO_4^{2-}). The bands at 1118 and 1145 cm^{-1} correspond to the vibration of antisymmetric elongation of the ions (SO_4^{2-}). The bands characteristic of the deformation vibration of water molecules are located at 1621 and 1685 cm^{-1} . Bands of symmetric and anti-symmetric elongation vibration of water molecules appear at 3244 , 3403 and 3549 cm^{-1} .

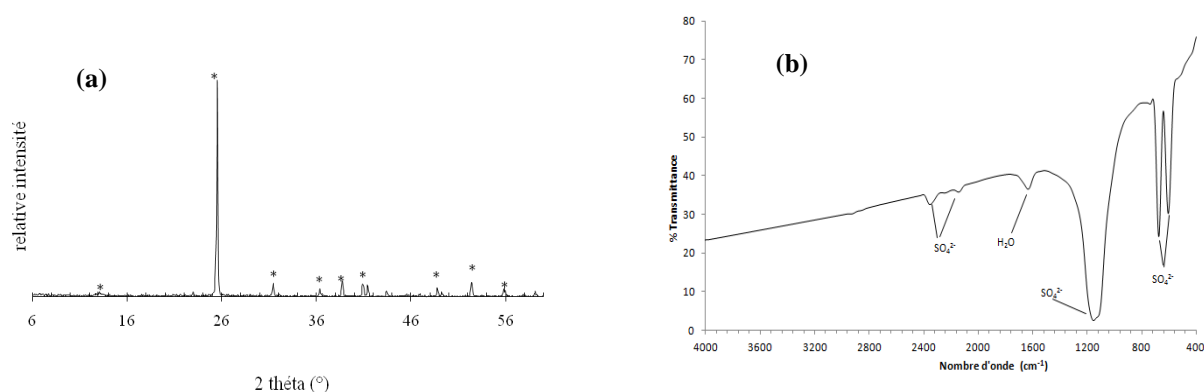


Figure 3: XRD patterns of the obtained anhydrite (a) and FT-IR patterns of the obtained anhydrite (b)

Figure 4 shows the XRD patterns of HAP particles derived from Moroccan PG at 105°C, 600°C and 900°C. All the diffraction peaks displayed in the XRD pattern were easily indexed to pure hexagonal structural HAP (space group P6₃/m) according to JCPDS card no. 09-0432. HAP dried at 105°C shows the presence of a significant amorphous phase. When the temperature increases to 600°C, several peaks of HAP become more distinct and narrow which suggests an increase in the degree of crystallinity. Figure 4 also shows that at 900°C, all the diffraction peaks were indexed to pure hexagonal structural HAP (space group P6₃/m) according to JCPDS card No. 09-0432 and exhibiting single major crystalline nature [22,23]. The only minor second phase observed is attributed to the presence of a small calcium oxide ICDD-PDF card N° 00-037 1497. The presence of CaO after heat treatment is in agreement with the results reported by other authors [24-26]. This can be explained by the fact that at higher temperatures carbonate groups are decomposed to emitted CO₂ and formed the calcium oxide CaO[27].

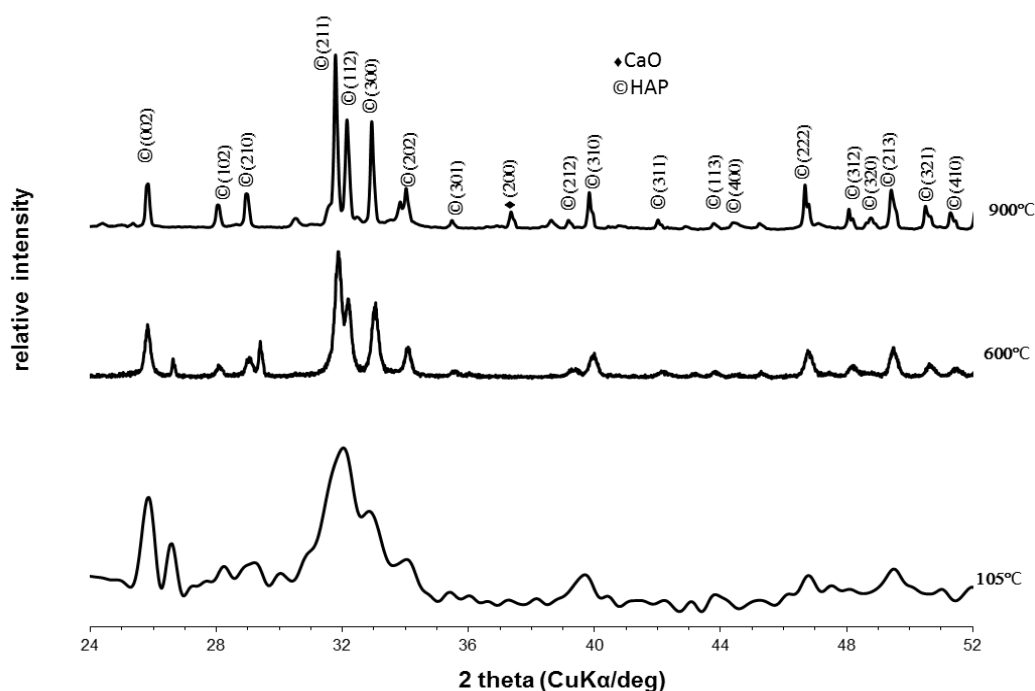


Figure 4: XRD patterns of HAP dried at 105°C (a), calcined at 600 °C (b) and 900 °C (c).

The FTIR spectra (Figure 5) of HAP powders before and after heat treatment at 600°C and 900°C shows all the peaks corresponding to OH and (PO₄)³⁻ stretching and no extra peak was observed. The broad peak between 3760 and 3000 cm⁻¹ corresponds to the hydrogen bonded O-H group stretch of HAP and water [28]. The three strong peaks at around 1040 cm⁻¹, 570 and 601 cm⁻¹ attributes to the P-O vibration modes. The band at 570 and 601 cm⁻¹ corresponds to the bending mode of (PO₄)³⁻ and the strong band at 1040 cm⁻¹ and 960 cm⁻¹ are due to the vibration of (PO₄)³⁻ group [29,30]. In addition, bands carbonate vibrations have also been observed around 1400 cm⁻¹ which indicates the absorption of carbon dioxide from atmosphere [31]. The absence of broadening of the peak at 1060 cm⁻¹ further confirms no decomposition of HAP to tricalcium phosphate β-Ca₃(PO₄)₂ at 900°C. The decrease in broadness of the peak between 3760 and 3000 cm⁻¹ with the increase in calcinations temperature indicates the removal of absorbed H₂O. From this analysis the formation of HAP is confirmed. The peaks are quite sharp at intermediate temperatures (600° C) and as the temperature increases peaks are going to be weak as shown in figure 5.

The DTA and GTA curves of dried HAP are illustrated in figure 6. The first and second steps occurred from 90 to 295°C with weight loss of 13.51% which represents the physical loss of both adsorbed and crystallization water [32,33]. The step occurred from 295 to 1000°C with 5.79% supposing to be the result of the gradual dehydroxylation of the HAP particles [34].

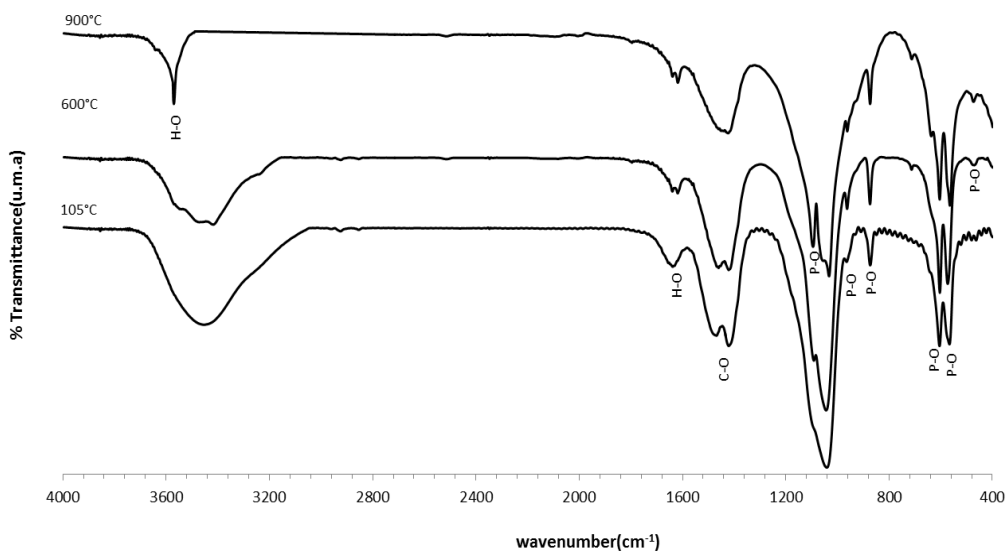


Figure 5: FT-IR spectra of dried HAP at 105°C (a), calcined HAP at 600°C (b) and at 900°C (c).

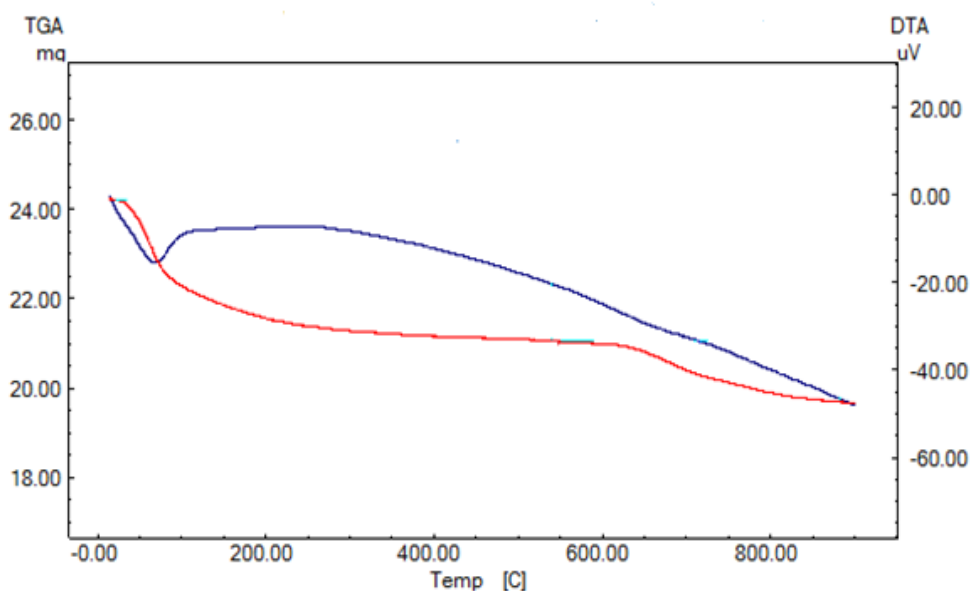


Figure 6: DTA-GTA curves of as-prepared HAP from Moroccan PG.

SEM images of HAP particles dried at 105°C and calcined at 600 °C and 900 °C are shown in figure 7. At 105°C powder particles of HAP were highly agglomerated, but in some areas, separate particles could be observed. The particle sizes varied from 5-20 nm and were of spherical-shaped. For calcined HAP sample at 600°C, the samples possess desultory structure and highly agglomerated containing mosaic of particles of different sizes and morphologies. The agglomeration of the particles is probably due to the ripening process [33].

However, in some areas good dispersion of particles could be observed. The particles were spherical-shaped and sizes ranged from 10 to 20 nm. SEM image of the powder calcined HAP at 900°C (Figure 7), revealed a slight increase in particle sizes compared to those calcined at lower temperatures. The particles of HAP become more uniform with especially spheroidal shape and homogeneous distribution. Figure 7c reveals presence of nanometric particles, the particle sizes were still of spherical-shaped and the sizes ranged from 0,1 to 0,4 µm.

The EDX spectrum (Figure 8) confirms the presence of calcium (Ca), phosphorus (P), oxygen (O) and trace of Na in the stoichiometric HAP sample. Chemical analysis (Table 3) show that the Ca/P ratio is equal to 1.667 which is close to 1,67 found in human bone and indicating stoichiometric HAP preparation. We can also see that the rates of metals: arsenic, cadmium, mercury and lead are in accordance with the ISO Standard 13779-2 concerning ceramic hydroxyapatite [35,36].

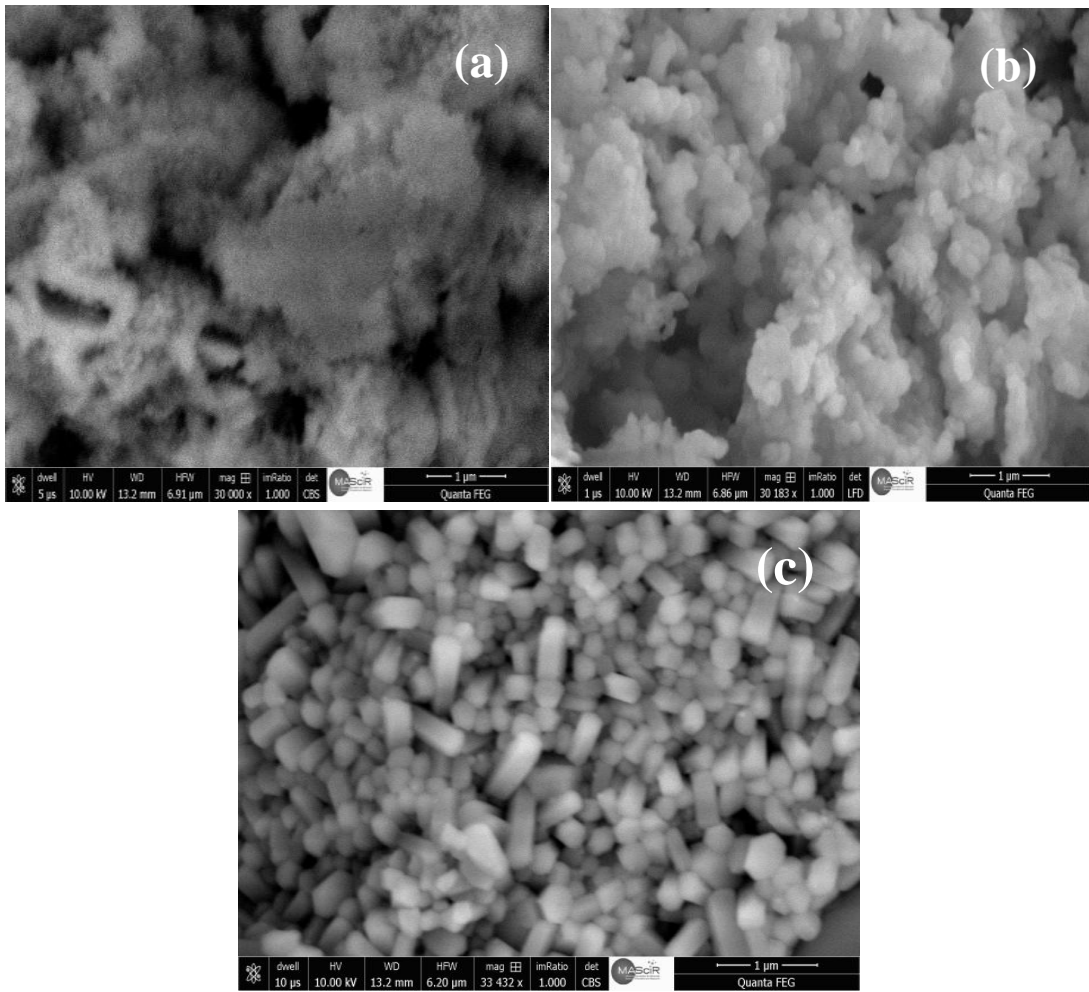


Figure 7: SEM images of dried HAP at 105 °C (a), calcined HAP at 600 °C (b) and 900 °C (c).

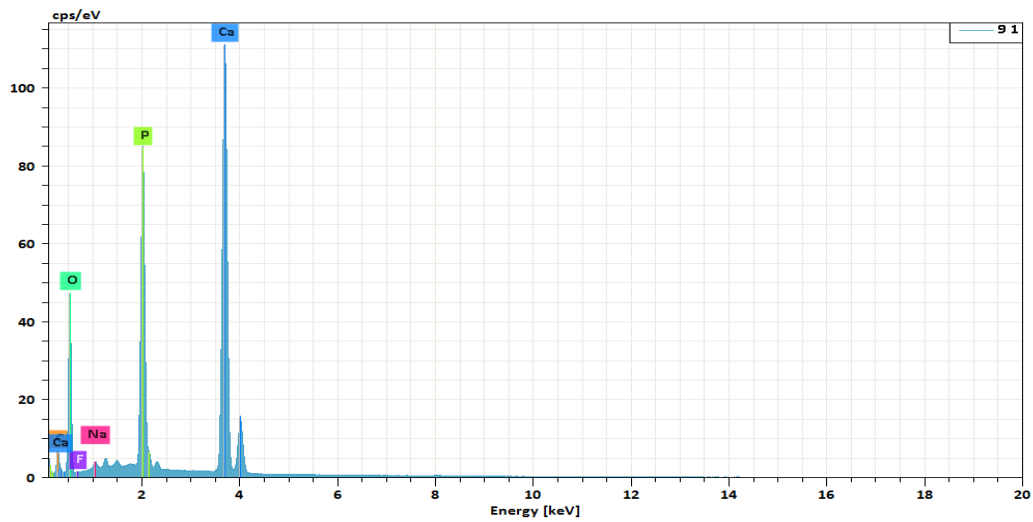


Figure 8: SEM-EDX of HAP powder.

Table 3: Chemical analysis of HAP particles at 105°C.

	%							Ppm					
	Ca	P	S	C	Na	F	Si	Ba	Mn	Ti	Pb	Sr	Zn
PG	23.05	0.40	18.04	0.14	0.10	0.12	0.25	66	3.6	996	1.66	811	5.76
HAP	33.45	15.51	0.00	0.21	0.13	0.03	0.00	55.66	0.72	940	0.89	523	2.76

Conclusion

Moroccan PG waste was first converted into anhydrite using a reactor made in our laboratory. Hydroxyde sodium was added to the anhydrite followed by phosphoric acid at room temperature. The proposed method leads to the obtaining of HAP with a Ca/P ratio equal to 1,667 which is close to 1,67 found in human bone and indicating stoichiometric HAP with a high degree of crystallinity, purity and a high yield. HAP derived from Moroccan PG can thus be applied for the treatment of liquid and gaseous effluents.

References

1. Rutherford P.M., Dudas M.J., *Sci. Total V Environ.* 180 (1996) 209
2. Singh M., Grag M., Verma C.L., Handa S.K, Umar R.K., *Constr. Build Mater.* 10 (1996) 600.
3. Ennaciri Y., Bettach M., Cherrat A., Zegzouti A., *J. Mater. Environ. Sci.* 7(6) (2016) 1925.
4. Tayibi H., Choura M., Lopez F.A., Alguacil F.J., Lopez-Delgado A., *J. Environ. Manage.* 90(8) (2009) 2377.
5. Bolivar J.P., Garcia-Tenorio R., Vaca F., *Water Res.* 34(11) (2000) 2941.
6. Degirmenci N., *Constr. Build. Mater.* 22 (2008) 1857.
7. Papastefanou C., Stoulos S., Ioannidou A., Manolopoulou M., *Environ. Radioact.* 89 (2006) 188.
8. Degirmenci N., Okucu A., Turabi A., *Build. Environ.* 42 (2007) 3393.
9. Zhang D., Luo H., Zheng L., Wang K., Li H., Wanga Y., Fenga H., *J Hazard Mater.* 241(2012) 418.
10. Mousa S.M., Ammar N.S., Ibrahim H.A., *J. Saudi Chem. Society (2016) 20, 357*
11. Chu T.M.G., Orton D.G., Hollister S. J., Feinberg S.E., Halloran J.W., *Biomater.* 23 (2002) 1283.
12. Hayati A.N., Rezaie H.R., Hosseinalipour S.M., *Mater. Lett.* 65 (2011) 736.
13. Baton J., Kadaksham A.J., Nzihou A., Singh P., Aubry N., *J. Hazard. Mater.* 139 (2007) 461.
14. Low H.R., Avdeev M., Ramesh K., White T. J., *Adv. Mater.* 24 (2012) 4175.
15. Baillez S., Nzihou A., Bernache-Assolant D., Champion E., Sharrock P., *J. Hazard. Mater.* 139 (2007) 446.
16. Lamzougui G., Nafai H., Bouhaouss A., Bchitou R., *J. Mater. Environ. Sci.* 7 (6) (2016) 2161-2169.
17. Chafik D., Bchitou R., Bouhaouss A., *J. Mater. Environ. Sci.* 5 (5) (2014) 1605-1610.
18. Hadioui M., Sharrock P., Mecherri M.O., Brumas V., Fiallo M., *Chem. Paper* 62 (2008) 516.
19. Zhang H., Liu M., Fan H., Zhang X., *Mater. Lett.* 75 (2012) 26.
20. Sanosh K.P., Chu M.C., Balakrishnan A., Lee Y.J, Kim T.N., Cho S.J., *Curr. Appl. Phys.* 9 (2009) 1459.
21. Nasrellah H., Loudiki A., El Gaini L., El Hajri J., El Krati M., Benkhouja K., Bakasse M., *Phys. Chem. News* 74, (2014) 76.
22. Chaudhry A.A., Haque S., Kellici S., Boldrin P., Rehman I., Khalid F.A., Darr J.A., *Chem. Commun.* 21 (2006) 2286.
23. Guo X., Wang W., Wu G., Zhang J., Mao C.,- Deng Y., Xi H., *New J. Chem.* 35 (2011) 663.
24. Lee D.K., Park J.Y., Kim M.R., Jang D.J., *Cryst. Eng. Comm.* 13 (2011) 5455.
25. Salimi M.N., Bridson R.H., Grover L.M., Leeke G.A., *Powder Technol.* 218 (2012) 109.
26. Predoi D., Vatasescu-Balcan R.A., Pasuk I., Trusca R., Costache M., *J. Optoelectron. Adv. Mater.*, 10(8) (2008) 2151
27. El Idrissia C B, Yamnib K, Yacoubia A, Massita A, *IOSR Journal of Applied Chemistry*, 7 (May. 2014) 107-112
28. Costescu A., Pasuk I., Ungureanu F., Dinischiotu A., Costache M., Huneau F., Galaup S., Le Coustumer P., Predoi D. *Dig. J. Nanomater. Biostruct.* (2010) 989
29. Qian J., Kang Y., Zhang W., Li Z., *J. Mater. Sci. Mater. Med.* 19 (2008) 3373.
30. Ciobanu C. S., Andronescu E., Vasile B.S., Valsangiacom C.M., Ghita R.V., Predoi D., *J. Optoelectron Adv. Mater.* 4 (2010) 1515.
31. Bai X., More K., Rouleau C. M., Rabiei A., *Acta Biomater.* 6 (2010) 2264.
32. Markovic M., Fowler B.O., Tung M.S., *J. Res. Nat. Inst. Stan.* 109 (2004) 553.
33. Mousa S., Hanna A., *Mater Res Bull.* 48 (2013) 823.
34. Monma H., Ueno S., Kanazawa T., *J. Chem. Technol. Biotechnol.* 31 (1981) 15.
35. Chandrasekar A., Sagadevan S., Dakshnamoorthy A., *Int. J. Phys. Sci.* 32 (2013) 1639.
36. Implants for Surgery-Hydroxyapatite: Coatings of Hydroxyapatite, in: British Standard, ISO 13779-2. 2nd edition (2008).

(2017) ; <http://www.jmaterenvironsci.com>